Neuron, Vol. 18, 779–791, May, 1997, Copyright ©1997 by Cell Press

Direct Evidence for Homotypic, Glia-Independent Neuronal Migration

Hynek Wichterle,* Jose Manuel García-Verdugo,† and Arturo Alvarez-Buylla*
*The Rockefeller University
New York, New York 10021
†Department of Cell Biology
Valencia University
Spain

Summary

Neuronal precursors born in the subventricular zone (SVZ) of the neonatal and adult rodent brain migrate 3–8 mm from the walls of the lateral ventricle into the olfactory bulb. This tangentially oriented migration occurs without the guidance of radial glia or axonal processes. The cells move closely associated, forming elongated aggregates called chains, which are ensheathed by astrocytes. We have developed a culture system in which postnatal mouse SVZ neuronal precursors assemble into chains with ultrastructural and immunocytochemical characteristics equivalent to those in vivo but without the astrocytic sheath. Time-lapse videomicrography revealed that individual cells migrate along the chains very rapidly (~122 μm/hr) in both directions. Periods of cell body translocation were interspersed with stationary periods. This saltatory behavior was similar to radial glia–guided migration but ~4 times faster. Neuronal precursors isolated from embryonic cortical ventricular zone or cerebellar external granule layer did not form chains under these conditions, suggesting that chain migration is characteristic of SVZ precursors. This study directly demonstrates that SVZ neuronal precursors migrate along each other without the assistance of astrocytes or other cell types. (Additional data are presented in www.cell.com).

Introduction

Neurons in the central nervous system are produced in restricted germinal layers frequently located millimeters away from their final destination. The accurate formation of brain cytoarchitecture and underlying neuronal connections depend on the ability of young neurons to migrate over long distances and to follow appropriate guidance cues. The best-studied form of neuronal migration is radial migration, in which neuronal precursors migrate away from restricted proliferative zones following the guiding processes of radial glia (Rakic, 1990). In vitro studies have demonstrated the translocation of young neurons moving along radial glial fibers (Edmondson and Hatten, 1987; Komuro and Rakic, 1995, 1996) and have helped to identify some molecules involved in radial migration (Rakic and Komuro, 1995; Zheng et al., 1996).

While many young neurons migrate radially, extensive tangential migration (i.e., perpendicular to the orientation of radial glia) of neuronal precursors has also been described (Rakic, 1990; O'Rourke et al., 1992, 1995; Walsh et al., 1992; Tan and Breen, 1993; Fishell et al., 1993). The mechanism of movement and the guidance of tangentially migrating precursors are poorly understood. One particularly striking example of tangential migration occurs in the anterior forebrain of neonatal and adult rodents (Luskin, 1993; Lois and Alvarez-Buylla, 1994). Neuronal precursors born in the subventricular zone (SVZ) of lateral ventricles migrate 3–8 mm tangentially through the SVZ (Doetsch and Alvarez-Buylla, 1996) and along its anterior extension, called the rostral migratory stream (RMS), to reach the olfactory bulb where they differentiate into granule and periglomerular neurons.

Interestingly, the SVZ cells in the adult brain do not follow radial glia or axonal guides. Instead, these cells migrate associated to each other, forming elongated cell aggregates resembling chains, inside tube-like structures formed by specialized astrocytes (Lois et al., 1996). This form of migration, called chain migration, carries large numbers of neuronal precursors along the RMS into the olfactory bulb at relatively high speeds (20–30 μm/hr) (Lois and Alvarez-Buylla, 1994; Luskin and Boone, 1994). The migrating SVZ cells express high levels of the polysialylated form of neural cell adhesion molecule (PSA-NCAM) (Bonfanti and Theodosis, 1994; Rousselot et al., 1995; Jankovski and Sotelo, 1996). Genetic deletion of PSA-NCAM (Tomasiewicz et al., 1993; Cremer et al., 1994) or enzymatic removal of polysialic acid from PSA-NCAM in wild-type mice (Ono et al., 1994) disrupts neuronal migration to the olfactory bulb. Interestingly, the NCAM mutant SVZ cells can migrate along the RMS of wild-type animals, indicating that the PSA-NCAM deficit is non-cell autonomous (Hu et al., 1996). Radial migration, in contrast to chain migration, is apparently not affected in the NCAM mutant mice. Together, these experiments suggest that cell–cell interaction is important for chain migration and that the mechanism of chain migration differs from radial migration.

The inference that neuronal precursors in the SVZ migrate associated to each other without radial glial or axonal guidance derives from ultrastructural reconstruction of the RMS. It is, however, not known how cells move within chains and what role ensheathing astrocytes play in chain migration. Here, we demonstrate the behavior of neuroblasts moving in chains using explant cultures of the SVZ. We show that SVZ cells in chains migrate long distances at high speeds by sliding along each other in the absence of glial cells.

Results

SVZ Cells Form Chains in a Three-Dimensional Extracellular Matrix Substrate

To establish optimal conditions for studying chain migration in vitro, we cultured SVZ explants from 5-day-old mice (P5) on different substrates. SVZ cells became organized as chains in Matrigel (Figure 1A), a three-dimensional extracellular matrix gel composed of collagen IV, laminin, heparan sulfate proteoglycans, and entactin–nidogen (Kleinman et al., 1982). In some cases,

For the movie, consult www.cell.com
The movie shows three sequences accelerated ~250 times.
Compact chain: Shows cells closely associated to each other in a chain. Only individual nuclei are visible. Notice how cells move along the chain in both directions. Six frames from this series are presented in Figure 6. The explant is to the lower right. Real time = 1 hr.
X chain: Shows the intersection formed by two chains and behavior of migrating cells in this intersection. Notice the cell that migrates along the upper left arm of the X and transfers in the intersection to the upper right arm. The explant is down. Real time = 1 hr.
Jumping cell: The proximal part of the culture where chains form a dense web. Notice the cell that transfers from one chain to a neighboring chain. During this exchange, the behavior of the leading process and growth cone is clearly displayed. The leading process extends, and the growth cone contacts a neighbor. At this time, the cell body that has been relatively quiescent translocates, crossing from one chain to the next. See also Figure 8. The explant is to the lower right. Real time = 1 hr.

individual long chains extending from an explant could be observed, while in others, cells formed a web of interconnected chains. Individual cells in chains were tightly apposed to each other. These chains were one to five cells wide and up to 600 μm long. Chains did not form on plastic, or on plastic coated with laminin (GIBCO), poly-D-lysine (GIBCO), fibronectin (GIBCO), or type IV collagen (Collaborative Research). The organization of cells in a gel prepared from type I collagen was similar to that described previously (Hu and Rutishauser, 1996; Hu et al., 1996). Migrating cells formed transient contacts with other cells and occasionally assembled into loose chains. However, in contrast to Matrigel, the majority of cells in collagen type I gel migrated as individual cells (Figure 1B). After 5 days in Matrigel, the chains began to fall apart, and cells either died, or some differentiated into neurons. The subsequent experiments were done in Matrigel within the first 3 days after explantation.

Only SVZ Cells Form Chains

Chains of migrating cells were observed in cultures of SVZ isolated from P1, P3, P5, P7, P10, P14, P20, and

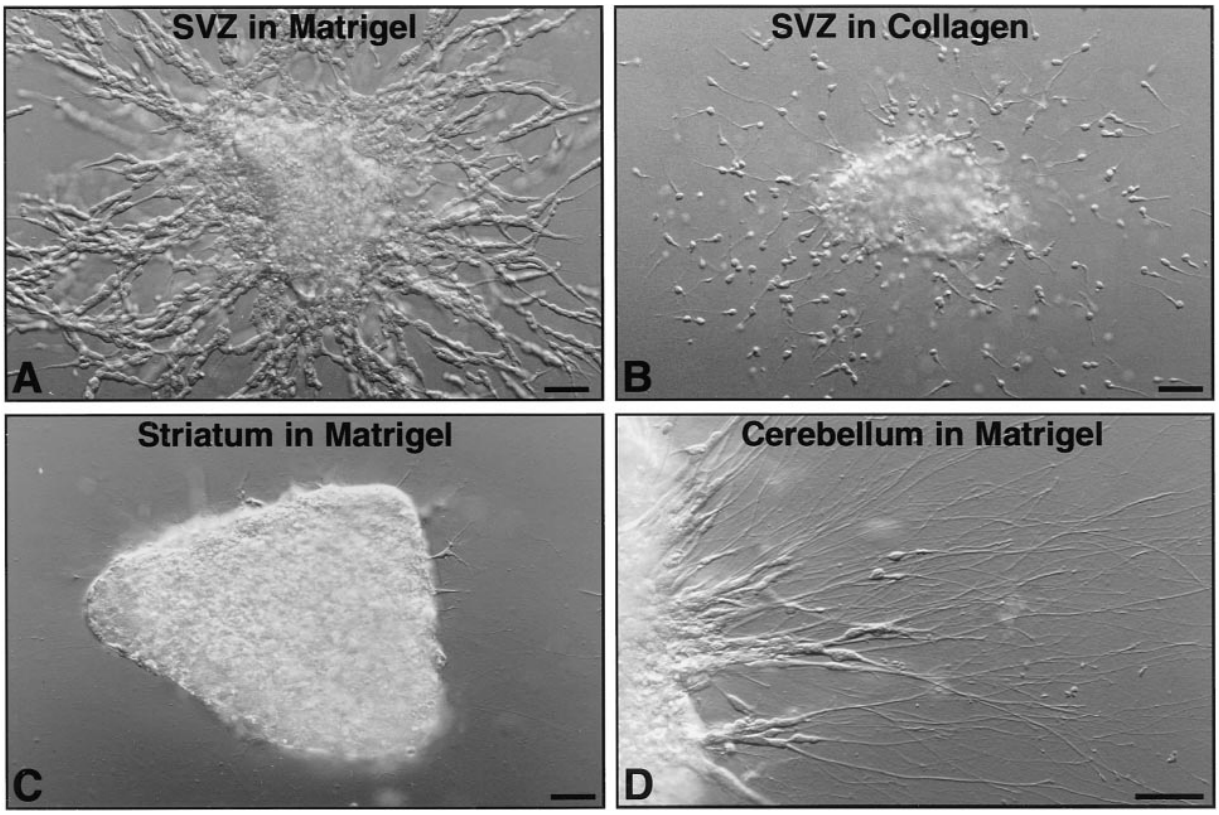

Figure 1. Explants from 5-Day-Old Mouse Brain Cultured on Different Substrates

(A) SVZ explants embedded in Matrigel formed a web of long interconnected chains around the explant.

(B) SVZ cells cultured inside a gel of collagen type I migrated away from the explant mostly as individual cells. Some chains were formed under this condition, but they were loose and transient, with individual cells becoming detached and migrating on their own.

(C) Explants of striatum without SVZ did not result in a cell outgrowth or the chain formation when cultured in Matrigel.

(D) Cells from cerebellar explants cultured in Matrigel migrated attached to long fibers.

(A and B) 24 hr in culture.

(C and D) 48 hr in culture. Scale bar = 50 μm.

2-month-old mice. An extensive and dense web of chains formed around SVZ explants isolated from P3–P10 mice, a period when the SVZ is largest and a time corresponding to the peak of neurogenesis in olfactory bulb interneurons (Hinds, 1968; Rosselli-Austin and Altman, 1995). For this reason, in most of the following experiments, we used explants of SVZ from P5 mice. To study whether chain formation is characteristic of SVZ cells or whether cells from other areas of the postnatal brain could also form chains, we prepared cultures of different postnatal (P5) mouse brain regions (striatum, medial septum, cortex, hippocampus, medial hypothalamus, and habenula). Very few cells emerged from these explants, and these cells were not organized as chains (Figure 1C). Since the majority of cells in these regions completed their migration soon after birth, we studied explants isolated from brain regions known to contain migrating cells. Two prominent sites of neuronal migration are the embryonic cortex (Angevine and Sidman, 1961) and the postnatal cerebellum (Rakic, 1985). Explants from embryonic day 15 (E15) cortical VZ or P5 cerebellar external granular layer in Matrigel did not result in chain formation. Instead, long fibers with closely attached cells (Figure 1D), resembling radially migrating neuronal precursors (Edmondson and Hatten, 1987; Komuro and Rakic, 1996), grew from cortical and cerebellar explants. Time-lapse video recording of cells along fibers from cerebellar explants revealed a migration similar to that previously described (Edmondson and Hatten, 1987) (data not shown).

Cells in Chains Correspond to Migrating Neuronal Precursors Observed In Vivo

Cells in chains were very closely attached to each other. Using differential interference contrast (DIC) microscopy, we distinguished individual cell nuclei, but it was generally not possible to discern the contour and shape of the entire cell. To visualize the morphology of individual cells in chains, crystals of DiI were mixed with explants so that only a small proportion of migrating cells were labeled. DiI-labeled cells in chains had an elongated morphology with a leading process 20–40 μm long and occasionally a thin trailing process (Figure 2B). The tip of the leading process extended into a growth cone with long, thin filopodia (arrow, Figures 2A and 2B). This cell morphology was very similar if not identical to that described in vivo for migrating cells along the RMS (Kishi, 1987).

To verify that these cells corresponded to the migrating neuronal precursors observed in vivo, we studied the chains by immunocytochemistry and electron microscopy. Cells in the chains were immunopositive for PSA-NCAM (Rougon et al., 1986) (Figures 2C and 2D) and TuJ1, a neuron-specific beta tubulin (Lee et al., 1990; Moody et al., 1996) (Figures 2E and 2F), two molecules present in the migrating neuronal precursors in vivo (Doetsch and Alvarez-Buylla, 1996). Chains did not contain vimentin-positive radial glial fibers or MAP2-positive neurites. Electron microscopy revealed that cells in chains were electron dense with elongated nuclei containing multiple nucleoli (Figure 3). Cells had many polyribosomes, bundles of microtubules in leading processes (Figure 3B), and pinocytic vesicles. This morphology was very similar to that described for type A cells, the migrating neuronal precursors in the RMS (Lois et al., 1996). Transverse sections of chains showed a close apposition of leading processes and cell bodies (Figures 3C and 3D). Electron microscopy did not reveal any glial fibers associated with studied chains.

Cells in Chains Are Not Ensheathed by Astrocytes

Whereas an extensive outgrowth of chains was observed around SVZ explants by 24 hr in culture, no glial fibrillary acidic protein (GFAP) immunoreactive cells were observed in the chains. However, beginning at 2 days after explantation, a few GFAP-positive (GFAP+) processes extended from explants (arrows, Figures 2G and 2H), and occasionally, GFAP+ cells were found associated with proximal segments of chains (arrowhead, Figures 2G and 2H). The number and length of GFAP immunoreactive fibers progressively increased with time in culture, but the distal segments of the chains were completely devoid of GFAP immunoreactivity even after 5 days in culture. Extensive network of chains formed even in cultures in which astrocytes were eliminated by treatment with 7B11 antibody recognizing an early astrocytic surface antigen (Szigeti and Miller, 1993) and a complement-mediated lysis, suggesting that the astrocytes are not required for chain formation (Figure 4).

Cells in Chains Migrate along Each Other

To determine the behavior of cells in chains, cultures were studied by time-lapse DIC videomicroscopy (movie at www.cell.com). DIC optics allowed us to visualize individual cell bodies within one focal plane of the three-dimensional cultures. Since cells deep in the Matrigel frequently move in and out of the focal plane, we mainly recorded chains that formed at the interface of the gel and the coverslip surface. Comparison of these chains with chains found deep in the Matrigel did not reveal any differences in cell morphology or behavior. Cells in chains were highly motile. Individual cells passed neighboring cells as they migrated through a chain (Figure 5; see also the movie). Even in very compact chains, individual cells migrated by literally sliding over their neighbors. Migration was bidirectional, with cells moving in opposite directions along the same chain (Figure 6). A few chains in which many actively migrating cells were observed were subsequently stained with anti-GFAP antibodies. No GFAP immunoreactive cell was detected in these chains, confirming that extensive movement of cells in chains occurs in the absence of astrocytes.

Migration of cells in chains consisted of cycles of rapid advancement interspersed with stationary periods (Figure 7 and Table 1). To study the displacement of individual cells, the position of the cell body of 22 moving cells (cells that within a 15 min sample period changed position) was recorded at 1 min intervals. The average velocity of these migrating cells was 122 μm/hr, and the average peak speed during active translocation was 302 μm/hr. Changes of cell body position as a function of time are shown in Figure 7 for four representative cells. Three of these cells migrated throughout the 45 min period with only short stationary periods, while the fourth cell became stationary at 4 min and resumed its

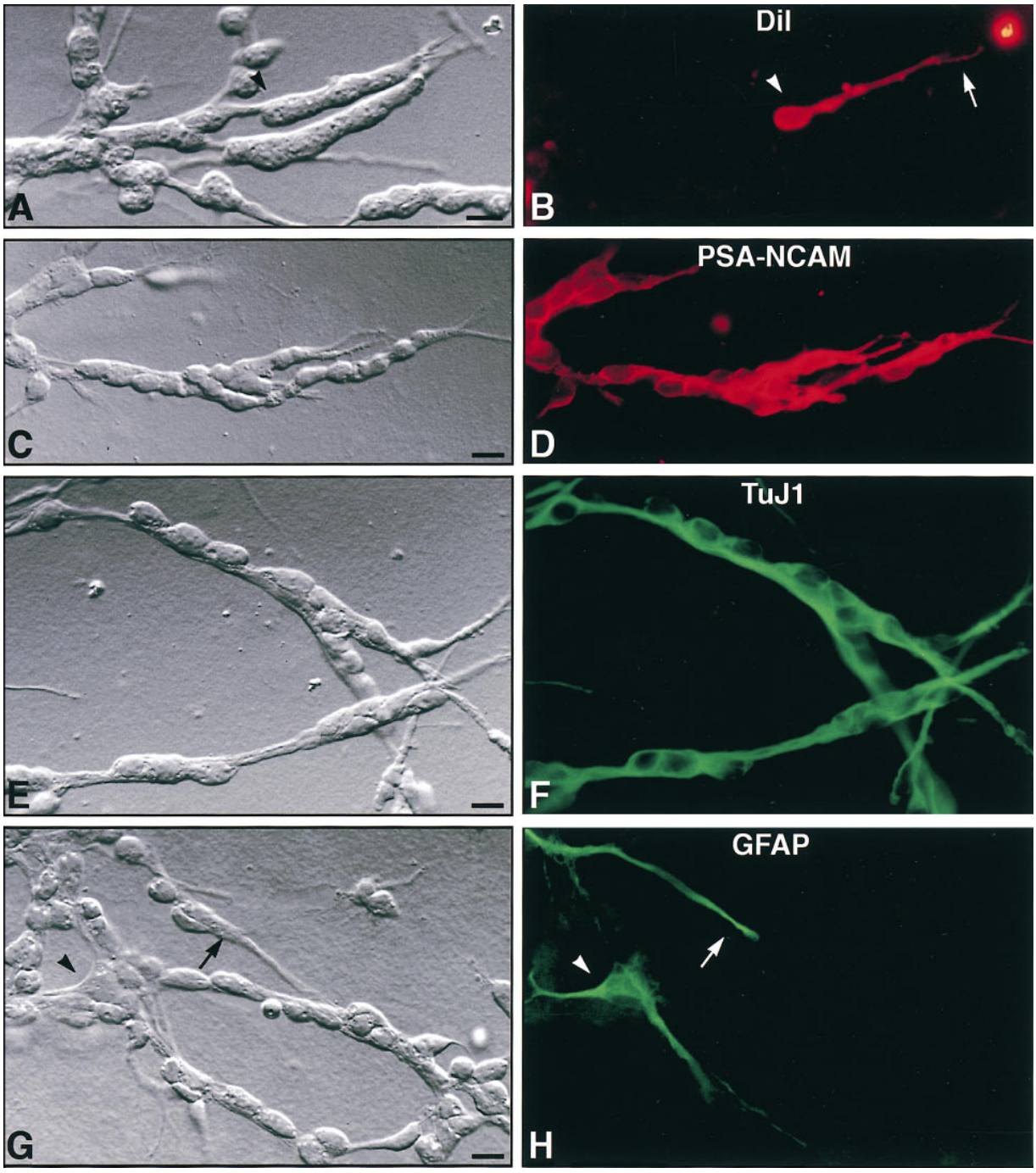

Figure 2. Morphological and Immunocytochemical Characterization of Cells in Chains

SVZ explants from P5 mice in Matrigel. (A), (C), (E), and (G) show DIC images; the corresponding fluorescent photomicrographs are shown on the right in (B), (D), (F), and (H). All pictures have the same orientation with the distal part of chains to the right.

(A and B) The morphology of individual cells in tightly packed chains was visualized by small crystals of lipophilic dye DiI added to the explant. An individual labeled cell (arrowhead) in a chain shows the elongated morphology with a leading process and a growth cone with long filopodia (arrow, [B]) that characterize migrating cells in the RMS. (The bright spot in the top right corner is a DiI crystal).

(C and D) Immunolabeling with antibodies against PSA-NCAM revealed that cells in chains were positive for this antigen.

(E and F) Cells in chains were also immunoreactive for the early neuronal marker TuJ1.

(G and H) Cells in the chains were immunonegative for GFAP. GFAP+ processes extended from explants to the proximal segments of chains (arrow). Occasionally, a GFAP+ astrocyte was observed associated to a chain (arrowhead). More distal parts of chains were devoid of GFAP immunoreactive processes.

(A–F) 24 hr in culture.

(G and H) 48 hr in culture. Scale bar = 10 μm.

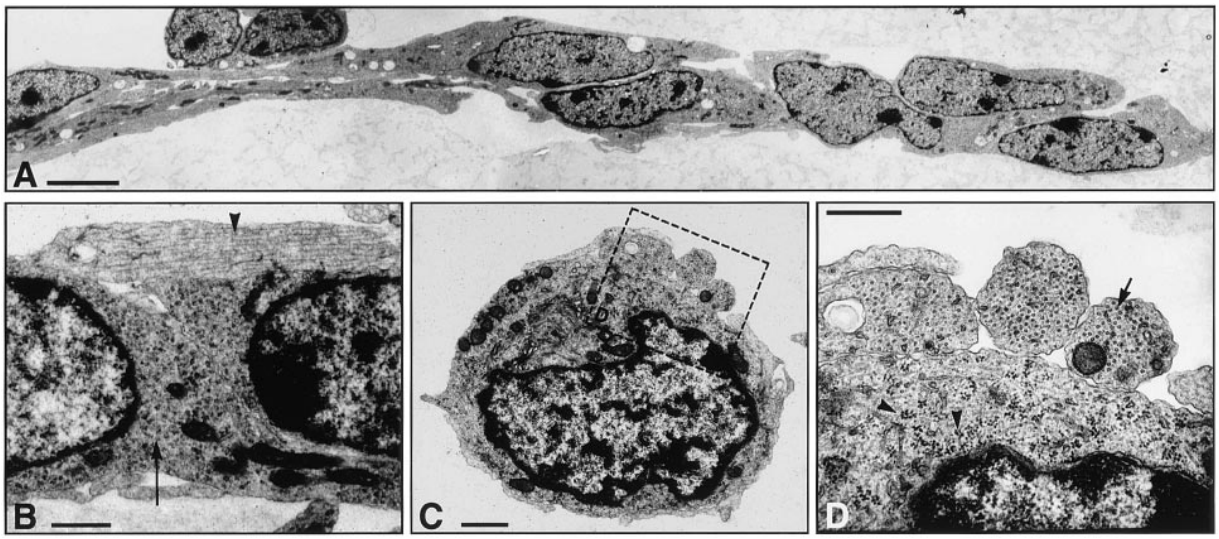

Figure 3. Ultrastructure of Cells in Chains (24 hr In Vitro)

(A) Chains were composed of electron-dense spindle-shaped cells with elongated nuclei containing sparse heterochromatin and several nucleoli. Individual cells were closely attached to each other. No axons or glial processes were encountered in the chains. Scale bar = 5 μm.

(B) Higher magnification of a portion of longitudinally cut chain shows association of two cells and a leading process. Notice the parallel arrays of microtubules (arrowhead) in the leading process. The cytoplasm is rich in polyribosomes (arrow) with scant rough endoplasmic reticulum. Scale bar = 1 μm.

(C) Transverse section of a chain showed close association of multiple leading processes with a cell body of another cell. Scale bar = 1 μm.

(D) Higher magnification of the transverse section shows the array of microtubules in the leading processes (arrow). The cytoplasm of cells close to the nuclei is rich in polyribosomes (arrowheads). Scale bar = 0.5 μm.

migration at 27 min. The average duration of each step was 4.1 min in which cells moved on average 19.4 μm, almost twice the soma length (91 steps analyzed from 22 cells). If we take into account only the moving cells (those that moved within the 15 min period), the duration of pauses was on average 2.2 min. To find out how many cells are migrating and how many are stationary, we analyzed all cells in one field in three independent cultures (885 cells studied) during 15 min periods at 22, 24, 25, 26, 27, 28, and 32 hr after explantation. Cells that did not move within these 15 min were considered stationary. The proportion of stationary and moving cells at these different times studied was very similar: there were 49.1 ± 6.4% stationary cells, 38.4 ± 8.0% of cells moving away from explants, and 12.5 ± 2.4% of cells moving toward explants. The speed of cell flow away from explants was determined in 15 chains to be 23.6 ± 9.2 μm/hr (the calculation is described in Experimental Procedures).

Mechanism of Translocation

The behavior of the growth cone and leading process during cell migration was difficult to analyze because cells in chains were usually tightly packed. However, on a few occasions, the leading process was clearly visible. This occurred in cultures in which chains formed a spread meshwork, or when cells moved from one chain to an adjacent one (Figure 8; see the jumping cell in the movie at www.cell.com). The dynamics of cell body translocation in these cases was similar to that of cells

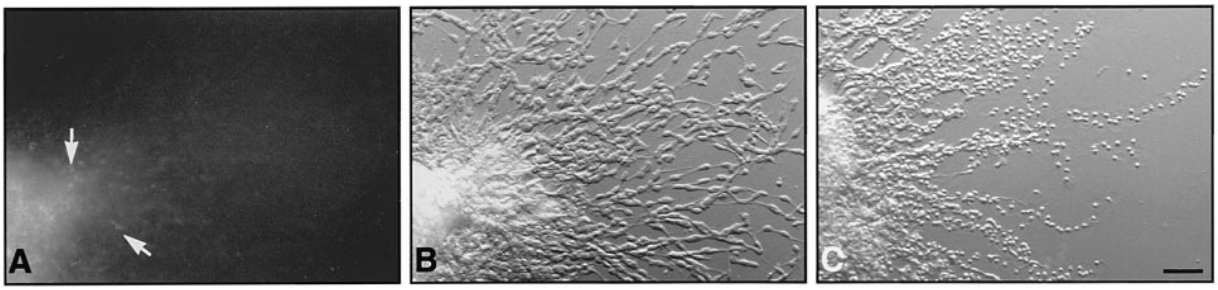

Figure 4. Chains Form Normally after Complement-Mediated Lysis of Astrocytes (48 Hr In Vitro)

(A and B) GFAP+ cells were eliminated from cultures by complement-mediated lysis of astrocytes with antibody 7B11. This treatment results in no GFAP+ cells or processes in chains. Some GFAP+ cell bodies remained inside the explant (arrows), but no GFAP+ fibers (Figure 2H) extended from these cells (A). Under these conditions, chains formed normally (B).

(C) In contrast, when cultures were preincubated with anti-PSA-NCAM antibodies, cells in chains were lysed by complement. Ghosts and rounded-up cell nuclei remain where the chains had extended before. For all panels, the scale bar = 50 μm.

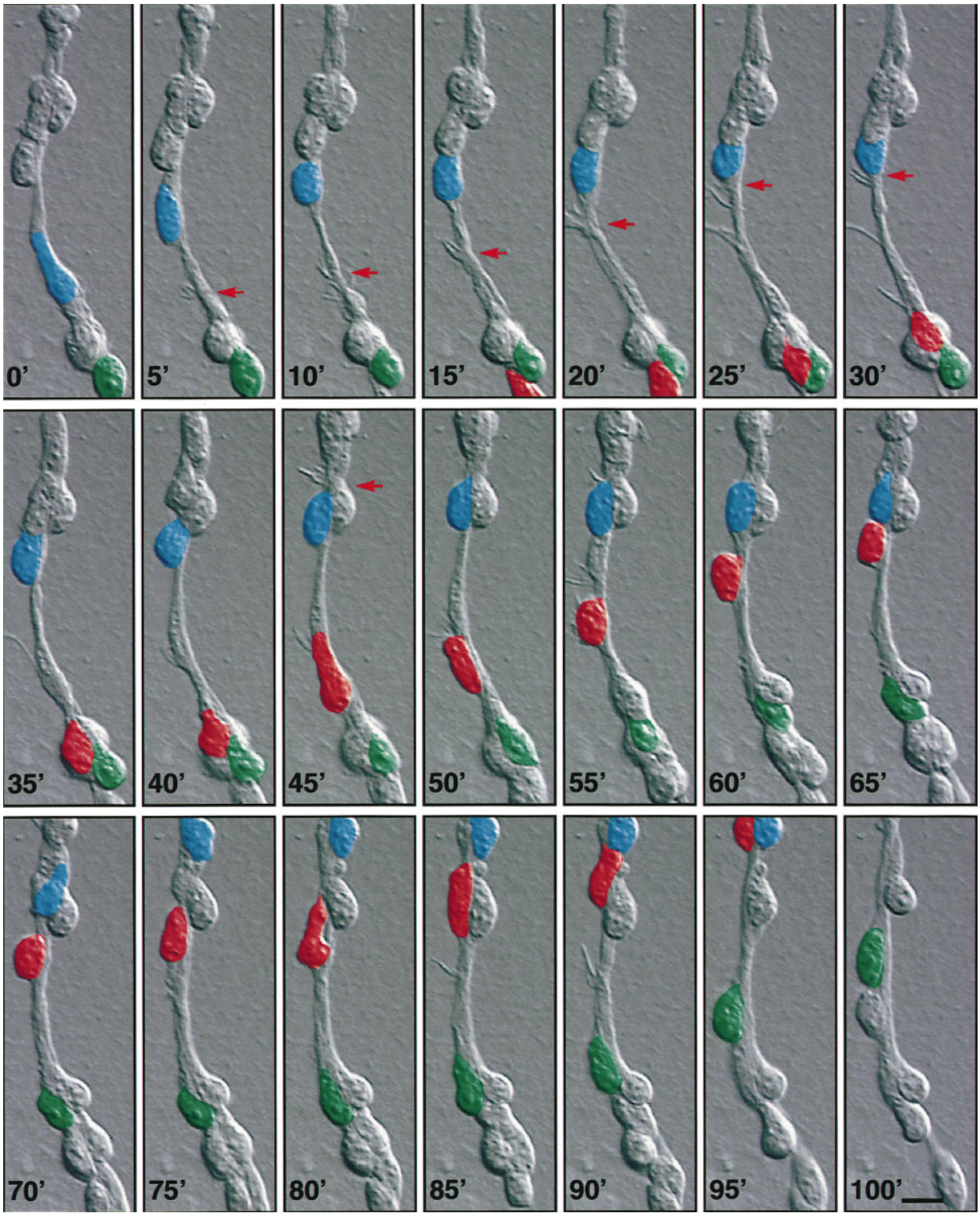

Figure 5. Time-Lapse Series Reveals Migration of Cells along the Chains

Behavior of cells in chains after 24 hr in culture was studied by time-lapse videomicrography. In this series, images of a chain were taken every 5 min for 100 min. Most cells in this chain moved away from the explant (toward the top). Three cells are highlighted in color (red, green, and blue) to show how the position of these cells changed. Whereas the corresponding leading process and growth cone of most cells in the chain cannot be distinguished, occasionally, some cells and their growth cones (arrow for the red cell's growth cone) could be identified in multiple images. Scale bar = 10 μm.

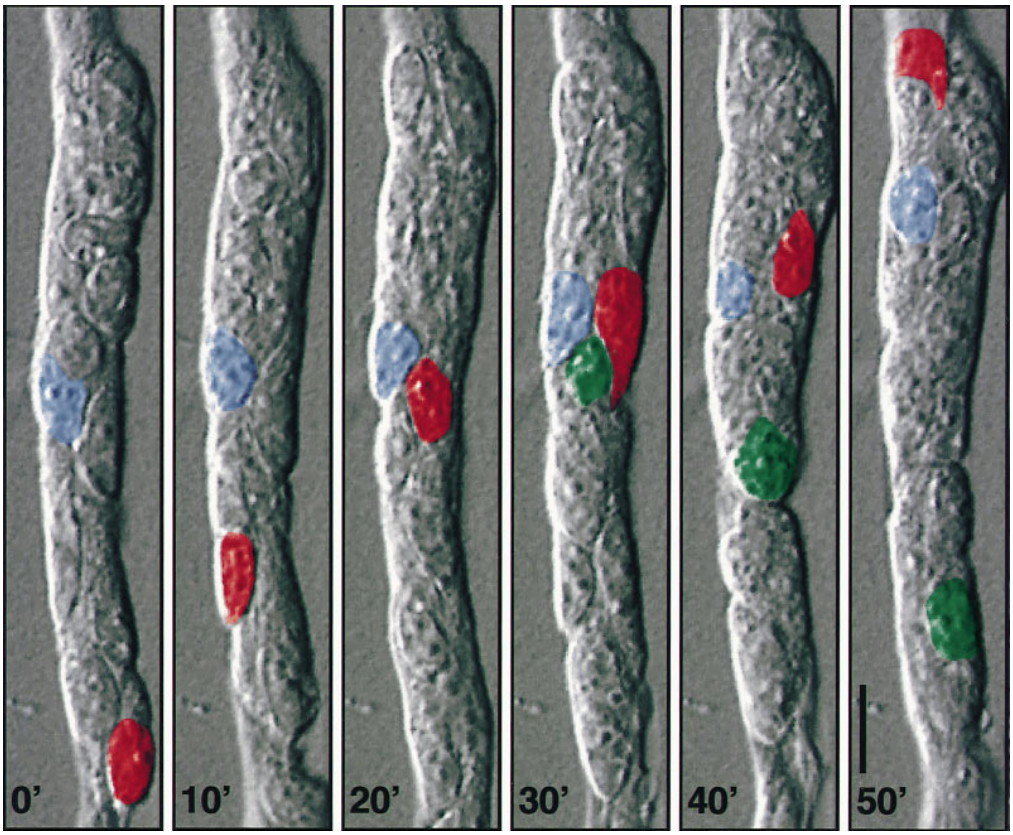

Figure 6. Time-Lapse Series Shows Bidirectional Movement in a Compact Chain (See Also the Movie)

Images were recorded every 10 min, and three cells are highlighted in color (red, green, and blue). The red cell moves rapidly away from the explant (toward the top), passing by the slowly moving blue cell. The green cell, which moved into the focal plane at 30 min, migrated toward the explant (bottom of the image). Scale bar = 10 μm.

in compact chains but allowed us to analyze in more detail the individual steps underlying chain migration. Similar behavior was observed in five other cells that were analyzed in this detail. Initially, the cell body was stationary, but the growth cone was extremely active as if exploring the territory by rapid extensions and retractions of long filopodia and short lamellae. The leading process could repeatedly extend and partially retract without a net change in the cell body position (Figure 9). This exploratory behavior lasted from a few minutes to several hours. Judging from the constancy in the maximum lengths of the leading process during several cycles of cell body translocation (Figure 9), there seemed to be a limited length that the leading process can attain. This maximal length is similar to that observed in vivo (Kishi, 1987; Lois and Alvarez-Buylla, 1994). Cell body translocation is generally initiated at the moment when the leading process is maximally extended and the movement of the nucleus correlates with a rapid shortening of the leading process (Figures 8C–F and 9). Occasionally, a thin trailing process is left behind the cell (arrowhead, Figure 8E), which rapidly retracts (Figure 8F). Cell body translocation is followed by another cycle of exploratory behavior during which the cell can again extend the leading process and proceed in migration, or alternatively, the cell can retract the leading process, become stationary, or change the orientation of its migration (data not shown).

Discussion

In this report, we provide the first direct evidence for migration of neuronal precursors along each other. This form of migration, called chain migration, is utilized by SVZ cells migrating to the olfactory bulb in postnatal and adult rodent brain (Lois et al., 1996). The present study shows that chain migration differs in several aspects from previously described radial glia–guided migration. First, glial cells are not required for this type of neuronal translocation, and second, chain migration is three to six times faster than glial-guided migration in vitro or in vivo.

Chain migration has been so far identified in the postnatal SVZ, which lies deep in the anterior forebrain, inaccessible to direct visualization. The objective of this study was to develop an in vitro system that would allow us to study the behavior and dynamic properties of individual neuronal precursors in the chains. Of several culture conditions tested, chains formed most readily in a three-dimensional gel composed of multiple extracellular components (Kleinman et al., 1982) (Matrigel). The ultrastructural and immunocytochemical analysis (PSA-NCAM, TuJ1 expression) showed that cells in these chains are equivalent to the migrating neuronal precursors in vivo, indicating that this in vitro model of chain migration is a fair representation of the process normally occurring in the brain. Moreover, only SVZ cells

Table 1. Comparison of Parameters Measured for Chain and Glial-Guided Migration In Vitro

	n	Chain ± SD	Radial ± SD*	Chain/Radial
Soma length [μm]	20	11.6 ± 2.1	12 ± 1.5	1.0
Soma width [μm]	20	5.6 ± 1.8	6 ± 1	0.9
Leading process length [μm]	26	29.3 ± 4.9	19 ± 3.5	1.5
Duration of step [min]	93	4.1 ± 1.7	4.8 ± 1.6	0.9
Duration of pause [min]	91	2.2 ± 2.6	4.3 ± 2.1	0.5
Step length [μm]	58	19.4 ± 7.0	4 ± 2	4.8
Maximum speed [μm/hr]	93	301.5 ± 134.7	56 ± 26	5.4
Average cell speed [μm/hr]	22	121.7 ± 37.3	33 ± 20	3.7

* Edmondson and Hatten, 1987

assembled as chains under these culture conditions. Neurons from other neurogenic regions outside the SVZ, such as the embryonic cortical VZ and postnatal cerebellar EGL, migrated attached to long fibers (Edmondson and Hatten, 1987; Komuro and Rakic, 1996) but did not form chains. These results suggest that chain migration is a characteristic feature of SVZ cells and that Matrigel provides a substrate conducive to chain formation in vitro.

Time-lapse videomicrography revealed that individual cells move within chains. Frequently, a cell would move in one direction while neighboring cells remained stationary or moved in the opposite direction. This suggests that chain migration results from individual cells sliding over each other, rather than from a cooperative motion of cohorts of cells.

The morphology of migrating cells was very similar to that observed in vivo (Kishi, 1987; Lois and Alvarez-Buylla, 1994), with an elongated cell body containing the nucleus and a leading process with a large growth

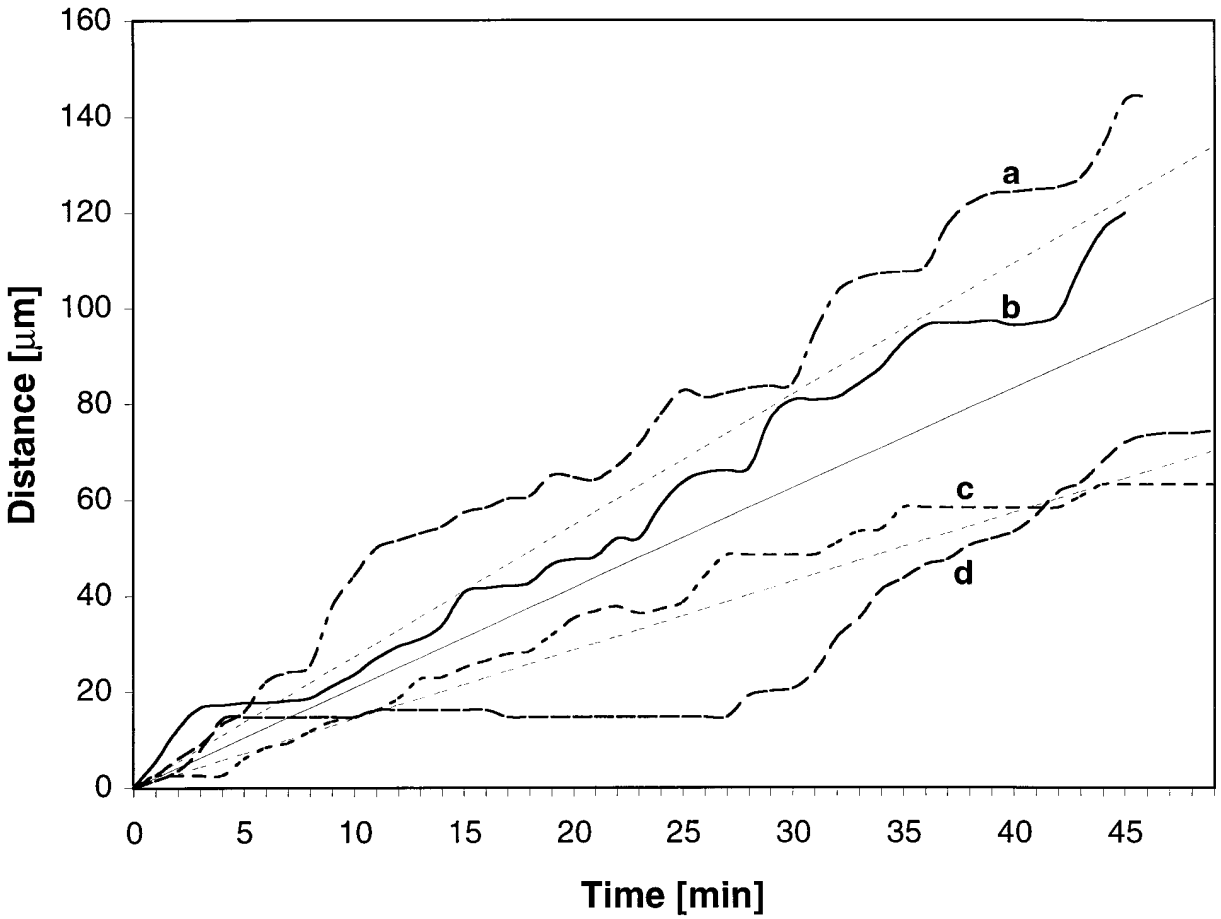

Figure 7. Saltatory Movement of a Cell Body during Migration

For this analysis, cell position was recorded in 1 min intervals and plotted as a function of time. The straight lines indicate the mean ± SD for 22 cells. The migratory profile of four representative cells (a, b, c, and d) shows the characteristic saltatory movement of these cells. Cells a, b, and c are considered to be migrating cells (stationary periods <15 min), while the fourth cell (d) became stationary at 4 min and resumed migration at 27 min.

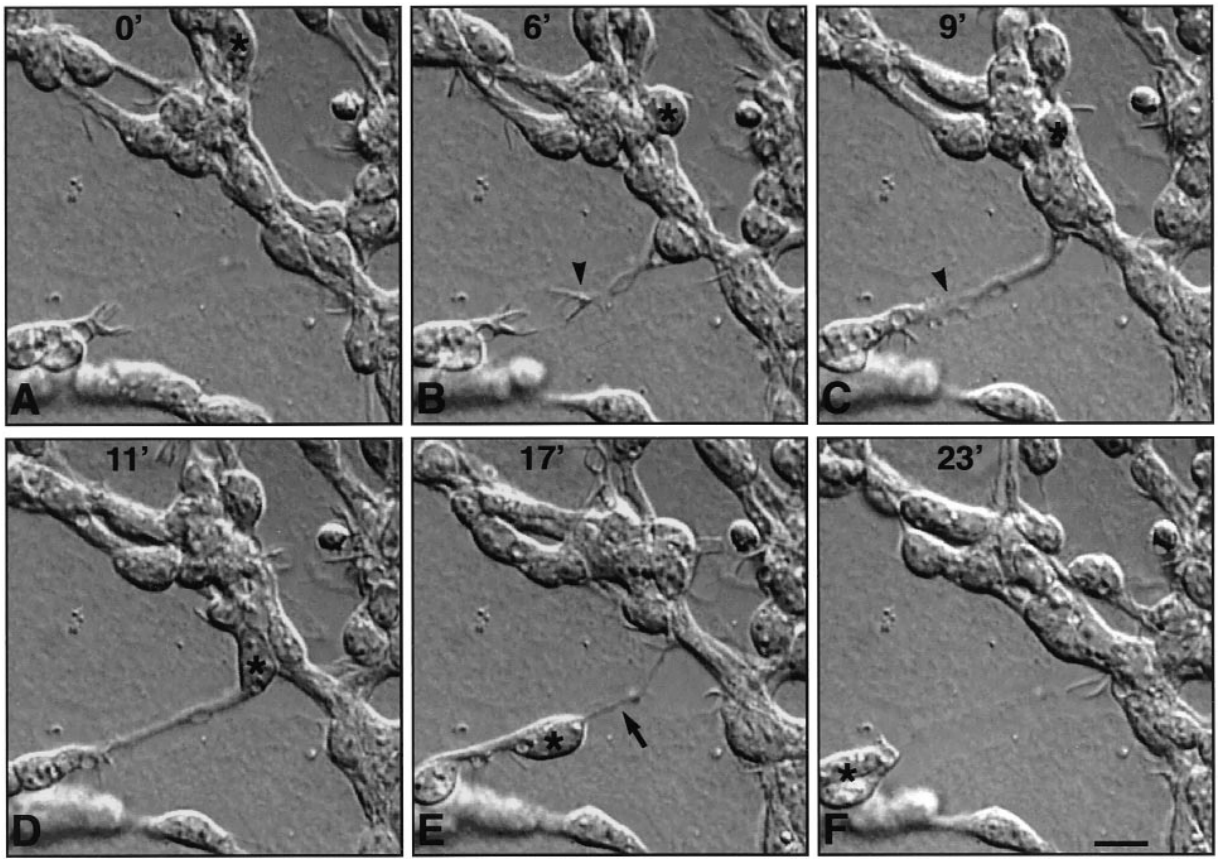

Figure 8. Time-Lapse Study of Cell Behavior during Translocation (See Also the Movie at www.cell.com)

This figure shows individual steps of cell body (star) translocation and behavior of a growth cone and leading process during cell movement between two parallel chains.

(A and B) The cell first extended the leading process with a highly motile growth cone (arrowhead) toward the second chain.

(C) A contact with a cell in the second chain was established (arrowhead).

(D–F) The cell body moved between the two chains. Notice the thin trailing process (arrow, [E]) that was rapidly retracted. Scale bar = 10 μm.

cone. Close examination of individual cells' behavior indicated that cell body movement correlated with a shortening of the leading process. The extension of the leading process may result in the accumulation of tension between the growth cone and cell body, resulting in the passive forward translocation of the cell body (Lamoreux et al., 1989; Heidemann and Buxbaum, 1994). Alternatively, when the leading process attains a certain length or the growth cone establishes a particular contact, a signal may be transmitted to the cell, resulting in the displacement of the nucleus and other organelles into the leading process. Periods of cell body translocation alternated with stationary periods during which the cell body did not move but the growth cone remained active. Interestingly, similar saltatory behavior has been observed in neuronal precursors migrating along glial fibers (Edmondson and Hatten, 1987; Komuro and Rakic, 1996). Recently, Komuro and Rakic showed that increases in cytosolic calcium in these cells coincide with periods of cell body translocation (Komuro and Rakic, 1996). Based on the analogous saltatory behavior and almost identical duration of migratory periods (~4–5 min) (Table 1), it is plausible that a similar calcium-mediated mechanism may be employed for cell body translocation during chain migration. Transient increases in intracellular calcium may trigger nucleus movement through an active mechanism involving molecular motors, or it may regulate the assembly and disassembly of microtubules in the leading process, resulting in a nucleus translocation (Rakic et al., 1996).

Although some aspects of chain migration and glial-guided migration may be simillar, there appear to be important differences. A cell migrating along a glial fiber has a long trailing process and a lamellar extension on the leading process that wraps around the guiding fiber (Rakic, 1972). A specialized interstitial junction (Gregory et al., 1988), which is thought to be important for cell body displacement and guidance, forms between the cell body and the guiding fiber. In contrast, none of these structures were observed in chain migrating cells in vitro or in vivo (Jankovski and Sotelo, 1996; Lois et al., 1996). The substrate for chain migration (other migrating cells) is discontinuous and motile, and the adhesive forces among individual cells are likely to be weak and transient, as individual cells could easily slide past each other even in very compact chains. These differences between radial migration and chain migration could explain the apparently selective hampering of chain migration in NCAM knockout mice (Tomasiewicz et al., 1993; Cremer et al., 1994) in which the loss of polysialylation

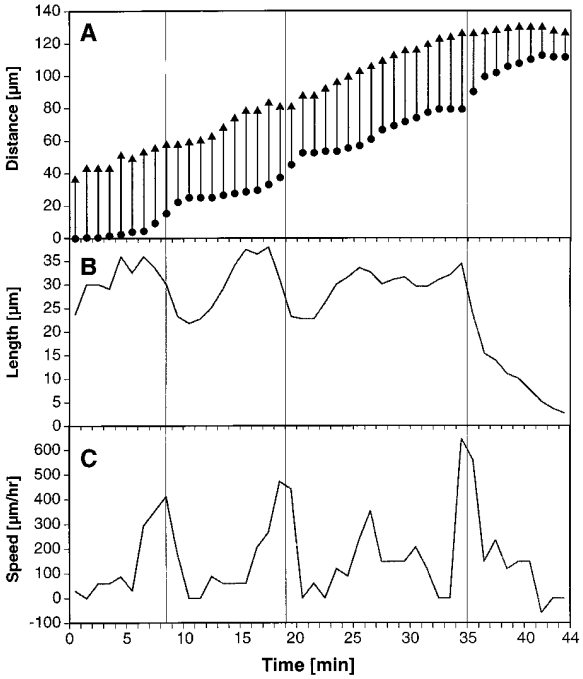

Figure 9. Correlation of Cell Body Speed and Leading Process Contraction

Behavior of a cell, for which we traced cell body as well as growth cone position, was studied in 1 min intervals during a 44 min period.
(A) The cell body (closed circle) and growth cone (arrowhead) positions as a function of time.
(B) The leading process length during the cell migration was calculated from cell body and growth cone positions.
(C) Speed of cell body translocation was calculated from distances between two consecutive cell body positions. Notice that periods of highest speed of cell body translocation correspond to periods of leading process contraction.

(PSA) prevents the migration along the RMS (Ono et al., 1994). PSA may be required to counteract adhesion of surface molecules (Hoffman and Edelman, 1983; Rutishauser et al., 1985) and allow plasticity in cell–cell contacts during chain migration. Our results suggest that the growth cones of migrating cells might act as the principal regions of firm contacts with substrate, serving as stable points supporting the intrinsic process of cell body translocation. In this sense, chain migration is more like growth of axons (Lamoreux et al., 1989; Heidemann and Buxbaum, 1994) but in which the cell bodies get carried along. Therefore, similar molecules, including PSA-NCAM, may be involved in both chain formation and axonal fasciculation (Dodd and Jessell, 1988; Rutishauser and Landmesser, 1991; Walsh and Doherty, 1991). The in vitro culture system developed here will allow further characterization of the molecular mechanisms underlying cell–cell interaction and cell translocation during chain migration.

Interestingly, the estimated speeds of chain migration in vivo (Lois and Alvarez-Buylla, 1994; Luskin and Boone, 1994) and in vitro are three to six times faster compared to cells moving along glial processes (Edmondson and Hatten, 1987; Jacobson, 1991) (Table 1). The tight apposition of migrating cells and glial fibers through lamellar extensions and interstitial junctions required for radial migration may also result in higher resistance to displacement. In contrast, the dynamic nature of contacts formed between cells during chain migration (allowing cells to change their partners constantly) might result in faster, less-restrained cell movement. Interestingly, chain migration was faster than tangential migration within the ventricular zone (10–100 μm/hr) (Fishell et al., 1993) or tangential migration in the developing intermediate zone of the cerebral cortex (24 μm/hr) (O'Rourke et al., 1992). Chain migration breaks all speed records in neuronal migration.

Chain migration in vivo is highly directional. The large majority of cells moving in the RMS are polarized with their leading process oriented toward the olfactory bulb (Kishi, 1987; Luskin, 1993; Lois and Alvarez-Buylla, 1994). Cells in culture, however, migrated bidirectionally along the chains. A cell moving in one direction may become stationary, change the orientation of the leading process, and resume migration in the opposite direction. Similar bidirectional migration has also been observed during glial-guided migration in vitro (Edmondson and Hatten, 1987). The mechanism that establishes and/or maintains a specific polarity of cells in vivo remains to be determined. It was recently suggested that a chemorepellent substance secreted from caudal septum may guide the rostral migration of SVZ precursors (Hu and Rutishauser, 1996). However, under the present culture conditions, we did not observe preferential direction of migration when SVZ explants were cocultured close (100–300 μm distance) to an explant of caudal or rostral septum, olfactory bulb, striatum, or cortex (results not shown). The fact that cells continue to migrate in vitro in the absence of directional cues suggests that directional signals are not required for cell translocation.

In the adult brain, chains of migrating neuronal precursors are ensheathed by GFAP+ astrocytes (Lois et al., 1996). This raised the question of whether ensheathing astrocytes are required for the formation of chains and for cell migration. In our cultures, the rapid movement of neuronal precursor occurred within the first 48 hr in vitro, when GFAP+ processes were found only in the proximal segments of some chains. Staining with anti-vimentin antibodies or electron microscopy analysis of these cultures did not show glial cells ensheathing these chains. Furthermore, elimination of astrocytes in cultures by complement-mediated lysis did not prevent chain formation and cell migration. This suggests that neuronal precursors could assemble into chains and migrate along each other without the assistance of ensheathing astrocytes. The glial cells are either not required for chain migration or signals normally provided by these cells were substituted by the three-dimensional culture substrate. Glial cells in vivo may play a role in isolating the migrating precursors from the surrounding brain parenchyma or could provide factors for the survival and directional migration of young neurons. It is interesting that GFAP+ cells and processes appearing in cultures at later stages were usually attached to the chains of neuronal precursors, suggesting that this in vitro system may allow future investigations of the role of the tube-like glial meshwork observed in vivo.

In this report, we demonstrated that young neurons in

the SVZ can migrate along each other. We characterized this form of neuronal migration and showed that it is distinct from previously described glial-guided migration. Glial-guided migration transports young neurons through a biochemically and anatomically discontinuous environment; e.g., from the germinal layer across the cell-poor and cell-rich brain parenchyma to the target region. The nature of chain migration, on the other hand, suggests that it is well suited for rapid transport of a large number of neurons across fairly uniform, cell-dense regions independent of radial glia. This opens the possibility that chain migration is not only utilized in postnatal and adult brain but may play an important role in cell dispersion during prenatal brain development. Several reports described tangential neuronal migration through embryonic germinal layers (Rakic and Sidman, 1969; Fishell et al., 1993) and developing cortex (Gadisseux et al., 1992; Menezes and Luskin, 1994; O'Rourke et al., 1995; De Carlos et al., 1996). It remains to be determined whether some embryonic neuroblasts migrate along each other in the same manner as demonstrated here for postnatal SVZ cells.

Experimental Procedures

Cultures of SVZ

Brains from 3- to 10-day-old CD-1 mice were placed in ice-cold Leibovitz's L-15 medium (GIBCO). The SVZ from the lateral wall of the anterior horn of lateral ventricle was dissected and cut into pieces 50–300 μm in diameter. The explants were mixed with Matrigel (Collaborative Biomedical Products) in a 1:3 ratio and allowed to congeal in a culture dish, which was prepared by cutting a 7.5 mm diameter hole in the bottom of a 35 mm petri dish (Corning) and attaching an 18 mm #1 coverslip with paraffin. The gel containing the explants was overlaid with 2 ml of serum-free Neurobasal medium (GIBCO) containing B-27 supplement (GIBCO), 0.5 mM L-glutamine (GIBCO), and penicillin–streptomycin antibiotics (GIBCO). Cultures were maintained in a humidified, 5% CO_2, 37°C incubator (Heraeus).

DiI Labeling

Crystals of lipophilic dye DiI (DiI, Molecular Probes) were inserted into explants of SVZ. Unincorporated crystals were washed off with excess of L-15 medium, and explants were embedded in Matrigel as described above. After 24 hr in culture, individual labeled cells were visualized with fluorescent illumination and photographed on an Olympus inverted microscope IX70.

Immunocytochemistry

Immunological characterization of cells in chains was performed directly in culture dishes. Samples were fixed with 3% paraformaldehyde solution in phosphate-buffered saline (PBS) (pH 7.3) for 1 hr at room temperature and blocked for 3 hr in 10% horse serum, 1% BSA, and 0.5% Triton X-100 in PBS. Incubation was with primary monoclonal antibodies (IgM anti-MEN-B to stain polysialylated N-CAM) (Rougon et al., 1986) (a gift from G. Rougon, Marseilles, France), 1:1000 dilution; TuJ1 (Lee et al., 1990; Moody et al., 1996), 1:500 dilution (a gift from A. Frankfurter, University of Virginia, Charlottesville); anti-GFAP (Sigma), 1:200 dilution; anti-vimentin 40E-C (Alvarez-Buylla et al., 1987) undiluted; and anti MAP2 (Sigma), 1:500 dilution, carried out overnight at 4°C. The samples were washed with 0.5% Triton X-100 in PBS and incubated either with goat anti-mouse IgM conjugated with RITC (to visualize anti-MEN-B antibodies and 40E-C) or with biotinylated horse anti-mouse IgG (Vector, 1:200 diluted) overnight at 4°C. After washing the cultures with 0.5% Triton X-100 in PBS, the biotinylated antibodies were visualized by incubating samples with FITC-conjugated avidin (Vector, 20 μg/ml) overnight at 4°C. Samples washed in 0.5% Triton X-100 in PBS were mounted in glycerol and photographed as described above.

Complement-Mediated Lysis

After 6 hr in vitro, cultures were incubated with 7B11 monoclonal antibody (Szigeti and Miller, 1993) (a gift from R. Miller, Case Western Reserve University, Cleveland) diluted 1:50 in medium for 2 hr at 37°C. Cultures were washed three times with medium and incubated with rabbit complement (Cappel), 1:5 dilution in medium for 2 hr at 37°C. Cultures were washed twice with medium. The procedure was repeated at 30 hr in vitro. The cultures were fixed after 48 hr in vitro and processed for GFAP immunoreactivity as described above. Explants incubated in anti-PSA-NCAM antibody diluted 1:1000 and complement under the same conditions as above resulted in the killing of cells in the chains (Figure 4).

Ultrastructural Analysis

Twenty-four hours after explantation, cultures were fixed in 3.5% glutaraldehyde for 30 min at 37°C; postfixed in 1% OsO_4 for 30 min at room temperature; stained in 5% aqueous uranyl acetate in the dark for 1 hr at 4°C; rinsed; dehydrated in ethanol; and infiltrated overnight in araldite (Durcupan, Fluka). Following polymerization, embedded cultures were detached from the coverslip by freezing in liquid nitrogen and thawing. Serial semithin (2 μm) and ultrathin (0.05 μm) sections were prepared in an Ultracut (Reichter), stained with lead citrate, and photographed on a Jeol 100CX electron microscope. In some cultures, the migrating cells studied by time-lapse videomicroscopy were subsequently identified at the electron microscope.

Time-Lapse Videomicrography

After 10–30 hr in culture, selected dishes were overlaid with 2 ml mineral oil (Sigma) and inserted into a heated culture chamber (Medical Systems Corp.). Steady flow (12.5 ml/min) of 100% CO_2 gas over the oil surface maintained neutral pH of the culture medium. The chamber was mounted on an inverted Olympus microscope equipped with Nomarski differential interference contrast optics and a monochromatic CCD camera Hitachi Denshi KP-M1U. Composite signal from the camera was recorded onto a Toshiba time-lapse video KV-6300A, set at 1:360 time compression and simultaneously captured into Power Macintosh 8500 at a rate of five frames/minute (1:360 time compression) at a resolution of 640 × 480 pixels, using Premiere 4.2 (Adobe) software. The cultures were recorded for periods ranging from 3–20 hr (www.cell.com).

Calculation of Cell Flow through a Chain

To calculate a bulk flow of cells through individual chains, we first counted how many cells migrating away from the explant pass an imaginary line across a selected chain (N_A) and the number of cells crossing the line migrating toward the explant (N_T) during a time period T. Rate of cell migration away from the explant was calculated as $(N_A - N_T)/T$. Next, we expressed thickness of the chain as the length of the chain corresponding to a single cell (L/C), where C is the number of cells contained in the chain of length L. The speed of bulk flow was then calculated by multiplying the rate of cell migration by the length of chain corresponding to a single cell: $((N_A - N_T)/T) * (L/C)$. Positive value of the calculated speed means that the overall cell movement is in the direction away from explants.

Acknowledgments

This work was supported by NIH Grant NS28478 to A.A.-B. H. W. is supported by a DeWitt Wallace/Reader's Digest fellowship. We thank A. Frankfurter, R. Miller, and G. Rougon for providing us with TuJ1, 7B11, and anti-PSA-NCAM antibodies, respectively. We are grateful to Daniel Lim, Fiona Doetsch, Enrique Font, Constance Scharff, Fernando Nottebohm, and Suzanna Ort for their useful comments on the manuscript and to the three anonymous reviewers for their suggestions.

Received February 20, 1997; revised April 22, 1997.

References

Alvarez-Buylla, A., Buskirk, D.R., and Nottebohm, F. (1987). Monoclonal antibody reveals radial glia in adult avian brain. J. Comp. Neurol. *264*, 159–170.

Angevine, J.B., Jr., and Sidman, R.L. (1961). Autoradiographic study of the cell migration during histogenesis of cerebral cortex in the mouse. Nature *192*, 766–768.

Bonfanti, L., and Theodosis, D.T. (1994). Expression of polysialylated neural cell adhesion molecule by proliferating cells in the subependymal layer of the adult rat, in its rostral extension and in the olfactory bulb. Neuroscience *62*, 291–305.

Cremer, H., Lange, R., Christoph, A., Plomann, M., Vopper, G., Roes, J., Brown, R., Baldwin, S., Kraemer, P., Scheff, S., Barthels, D., Rajewsky, K., and Wille, W. (1994). Inactivation of the N-CAM gene in mice results in size reduction of the olfactory bulb and deficits in spatial learning. Nature *367*, 455–459.

De Carlos, J.A., Lopez-Mascaraque, L., and Valverde, F. (1996). Dynamics of cell migration from the lateral ganglionic eminence in the rat. J. Neurosci. *16*, 6146–6156.

Dodd, J., and Jessell, T.M. (1988). Axon guidance and the patterning of neuronal projections in vertebrates. Science *242*, 692–699.

Doetsch, F., and Alvarez-Buylla, A. (1996). Network of tangential pathways for neuronal migration in adult mammalian brain. Proc. Natl. Acad. Sci. USA *93*, 14895–14900.

Edmondson, J.C., and Hatten, M.E. (1987). Glial-guided granule neuron migration in vitro: a high-resolution time-lapse video microscopic study. J. Neurosci. *7*, 1928–1934.

Fishell, G., Mason, C.A., and Hatten, M.E. (1993). Dispersion of neural progenitors within the germinal zones of the forebrain. Nature *362*, 636–638.

Gadisseux, J.-F., Goffinet, A.M., Lyon, G., and Evrard, P. (1992). The human transient supbial granular layer: an optical, immunohistochemical, and ultrastructural analysis. J. Comp. Neurol. *324*, 94–114.

Gregory, W.A., Edmondson, J.C., Hatten, M.E., and Mason, C.A. (1988). Cytology and neuron-glial apposition of migrating cerebellar granule cells in vitro. J. Neurosci. *8*, 1728–1738.

Heidemann, S.R., and Buxbaum, R.E. (1994). Mechanical tension as a regulator of axonal development. Neurotoxicology *15*, 95–107.

Hinds, J.W. (1968). Autoradiographic study of histogenesis in the mouse olfactory bulb. I. Time of origin of neurons and neuroglia. J. Comp. Neurol. *134*, 287–304.

Hoffman, S., and Edelman, G.M. (1983). Kinetics of homophilic binding by embryonic and adult forms of the neural cell adhesion molecule. Proc. Natl. Acad. Sci. USA *80*, 5762–5766.

Hu, H.Y., and Rutishauser, U. (1996). A septum-derived chemorepulsive factor for migrating olfactory interneuron precursors. Neuron *16*, 933–940.

Hu, H.Y., Tomasiewicz, H., Magnuson, T., and Rutishauser, U. (1996). The role of polysialic acid in migration of olfactory bulb interneuron precursors in the subventricular zone. Neuron *16*, 735–743.

Jacobson, M. (1991). Developmental Neurobiology (New York: Plenum Press).

Jankovski, A., and Sotelo, C. (1996). Subventricular zone–olfactory bulb migratory pathway in the adult mouse: Cellular composition and specificity as determined by heterochronic and heterotopic transplantation. J. Comp. Neurol. *371*, 376–396.

Kishi, K. (1987). Golgi studies on the development of granule cells of the rat olfactory bulb with reference to migration in the subependymal layer. J. Comp. Neurol. *258*, 112–124.

Kleinman, H.K., McGarvey, M.L., Liotta, L.A., Robey, P.G., Tryggvason, K., and Martin, G.R. (1982). Isolation and characterization of type IV procollagen, laminin, and heparan sulfate proteoglycan from the EHS sarcoma. Biochemistry *21*, 6188–6193.

Komuro, H., and Rakic, P. (1995). Dynamics of granule cell migration: a confocal microscopic study in acute cerebellar slice preparations. J. Neurosci. *15*, 1110–1120.

Komuro, H., and Rakic, P. (1996). Intracellular Ca^{2+} fluctuations modulate the rate of neuronal migration. Neuron *17*, 275–285.

Lamoreux, P., Buxbaum, R.E., and Heidemann, S.R. (1989). Direct evidence that growth cones pull. Nature *340*, 159–162.

Lee, M.K., Tuttle, J.B., Rebhun, L.I., Cleveland, D.W., and Frankfurter, A. (1990). The expression and posttranslational modification of a neuron-specific b-tubulin isotype during chick embryogenesis. Cell Motil. Cytoskeleton *17*, 118–132.

Lois, C., and Alvarez-Buylla, A. (1994). Long-distance neuronal migration in the adult mammalian brain. Science *264*, 1145–1148.

Lois, C., Garcia-Verdugo, J.M., and Alvarez-Buylla, A. (1996). Chain migration of neuronal precursors. Science *271*, 978–981.

Luskin, M.B. (1993). Restricted proliferation and migration of postnatally generated neurons derived from the forebrain subventricular zone. Neuron *11*, 173–189.

Luskin, M.B., and Boone, M.S. (1994). Rate and pattern of migration of lineally-related olfactory bulb interneurons generated postnatally in the subventricular zone of the rat. Chem. Senses *19*, 695–714.

Menezes, J.R.L., and Luskin, M.B. (1994). Expression of neuron-specific tubulin defines a novel population in the proliferative layers of the developing telencephalon. J. Neurosci. *14*, 5399–5416.

Moody, S.A., Miller, V., Spanos, A., and Frankfurter, A. (1996). Developmental expression of a neuron-specific b-tubulin in frog (*Xenopus laevis*): a marker for growing axons during the embryonic period. J. Comp. Neurol. *364*, 219–230.

Ono, K., Tomasiewicz, H., Magnuson, T., and Rutishauser, U. (1994). N-CAM mutation inhibits tangential neuronal migration and is phenocopied by enzymatic removal of polysialic acid. Neuron *13*, 595–609.

O'Rourke, N.A., Dailey, M.E., Smith, S.J., and McConnell, S.K. (1992). Diverse migratory pathways in the developing cerebral cortex. Science *258*, 299–302.

O'Rourke, N.A., Sullivan, D.P., Kaznowski, C.E., Jacobs, A.A., and McConnell, S.K. (1995). Tangential migration of neurons in the developing cerebral cortex. Development *121*, 2165–2176.

Rakic, P. (1972). Mode of cell migration to the superficial layers of fetal monkey neocortex. J. Comp. Neurol. *145*, 61–84.

Rakic, P. (1985). Mechanisms of neuronal migration in developing cerebellar cortex. In Molecular Basis of Neuronal Development, G.M. Edelman, W. E. Gall, and W. M. Cowan, eds. (New York: Wiley), pp. 139–159.

Rakic, P. (1990). Principles of neural cell migration. Experientia *46*, 882–891.

Rakic, P., and Sidman, R.L. (1969). Telencephalic origin of pulvinar neurons in the fetal human brain. Z. Anat. Entwickl. -Gesch. *129*, 53–82.

Rakic, P., and Komuro, H. (1995). The role of receptor/channel activity in neuronal cell migration. J. Neurobiol. *26*, 299–315.

Rakic, P., Knyihar-Csillik, E., and Csillik, B. (1996). Polarity of microtubule assemblies during neuronal cell migration. Proc. Natl. Acad. Sci. USA *93*, 9218–9222.

Rosselli-Austin, L., and Altman, J. (1995). The postnatal development of the main olfactory bulb of the rat. J. Dev. Physiol. *1*, 295–313.

Rougon, G., Dubois, C., Buckley, N., Magnani, J.L., and Zollinger, W. (1986). A monoclonal antibody against Meningococcus Group B polysaccharides distinguishes embryonic from adult N-CAM. J. Cell Biol. *103*, 2429–2437.

Rousselot, P., Lois, C., and Alvarez-Buylla, A. (1995). Embryonic (PSA) N-CAM reveals chains of migrating neuroblasts between the lateral ventricle and the olfactory bulb of adult mice. J. Comp. Neurol. *351*, 51–61.

Rutishauser, U., and Landmesser, L. (1991). Polysialic acid on the surface of axons regulates patterns of normal and activity-dependent innervation. Trends Neurosci. *14*, 528–532.

Rutishauser, U., Watanabe, M., Silver, J., Troy, F.A., and Vimr, E.R. (1985). Specific alteration of NCAM-mediated cell adhesion by an endoneuraminidase. J. Cell Biol. *101*, 1842–1849.

Szigeti, V., and Miller, R.H. (1993). A cell surface antigen expressed by astrocytes and their precursors. GLIA *8*, 20–32.

Tan, S-S., and Breen, S. (1993). Radial mosaicism and tangential cell dispersion both contribute to mouse neocortical development. Nature *362*, 638–639.

Tomasiewicz, H., Ono, K., Yee, D., Thompson, C., Goridis, C., Rutishauser, U., and Magnuson, T. (1993). Genetic deletion of a neural cell adhesion molecule variant (N-CAM 180) produces distinct defects in the central nervous system. Neuron *11*, 1163–1174.

Walsh, F.S., and Doherty, P. (1991). Glycosylphosphatidylinositol

anchored recognition molecules that function in axonal fasciculation, growth and guidance in the nervous system. Cell Biol. Int. Rep. *15*, 1151–1166.

Walsh, C., Cepko, C.L., Ryder, E.F., Church, G.M., and Tabin, C. (1992). The dispersion of neuronal clones across the cerebral cortex. Science *258*, 317–320.

Zheng, C., Heintz, N., and Hatten, M.E. (1996). CNS gene encoding astrotactin, which supports neuronal migration along glial fibers. Science *272*, 417–419.